Bio-precipitation of uranium by two bacterial isolates recovered from extreme environments as estimated by potentiometric titration, TEM and X-ray absorption spectroscopic analyses

Mohamed L. Merroun[a,b]*, Marta Nedelkova[a#], Jesus J. Ojeda[c,d], Thomas Reitz[a§], Margarita López Fernández[b], José M. Arias[b], María Romero-González[c], Sonja Selenska-Pobell[a]

[a]Institute of Radiochemistry, Helmholtz Centre Dresden-Rossendorf, Dresden, Germany

[b]Departamento de Microbiología, Universidad de Granada, Campus Fuentenueva s/n 18071, Granada Spain

[c] Cell-Mineral Interface Research Programme, Kroto Research Institute, University of Sheffield, Broad Lane, Sheffield, S3 7HQ, UK

[d] Experimental Techniques Centre, Brunel University, Uxbridge, Middlesex, UB8 3PH, UK

Present address:

[#] Biotechnologisches Zentrum, Technical University of Dresden, Dresden, Germany

[§] Department of Soil Ecology, Helmholtz Centre for Environmental Research – UFZ, Theodor-Lieser Strasse 4, 06120 Halle, Germany

*Corresponding author at: Tel: + 34 958 249331, fax: + 34 958 249486

E-mail adress: merroun@ugr.es (M.L. Merroun)

ABSTRACT

This work describes the mechanisms of uranium biomineralization at acidic conditions by *Bacillus sphaericus* JG-7B and *Sphingomonas* sp. S15-S1 both recovered from extreme environments. The U-bacterial interaction experiments were performed at low pH values (2.0-4.5) where the uranium aqueous speciation is dominated by highly mobile uranyl ions. X-ray absorption spectroscopy (XAS) showed that the cells of the studied strains precipitated uranium at pH 3.0 and 4.5 as a uranium phosphate mineral phase belonging to the meta-autunite group. Transmission electron microscopic (TEM) analyses showed strain-specific localization of the uranium precipitates. In the case of *B. sphaericus* JG-7B, the U(VI) precipitate was bound to the cell wall. Whereas for *Sphingomonas* sp. S15-S1, the U(VI) precipitates were observed both on the cell surface and intracellularly. The observed U(VI) biomineralization was associated with the activity of indigenous acid phosphatase detected at these pH values in the absence of an organic phosphate substrate. The biomineralization of uranium was not observed at pH 2.0, and U(VI) formed complexes with organophosphate ligands from the cells. This study increases the number of bacterial strains that have been demonstrated to precipitate uranium phosphates at acidic conditions via the activity of acid phosphatase.

Keywords: Uranium biomineralization; potentiometric titration; XAS; TEM/EDX; acid phosphatase

1. Introduction

Uranium is a long-lived, naturally occurring radionuclide that is an ecological contaminant and a human health hazard. The main sources of U pollution include mining activities, manufacture of nuclear weapons, nuclear energy production, and storage of radioactive wastes [1]. In Eastern Germany, the majority of U mining activities were concentrated in Saxony and Thuringia and produced 220.000 metric tons of U starting from 1946 until 1991[2]. These operations ended due to financial and political causes resulting in the accumulation of abandoned contaminated mine works with a subsurface void volume greater than 10^8 m^3. In addition, 5 x 10^8 tons of radioactive mining waste was spread over 3000 piles and 20 tailings in densely populated areas [2]. These U contaminated sites need a long-term stewardship in addition to remediation.

The microbial based remediation of environmental metal pollution offers an efficient and cheap alternative to the commonly used physicochemical approaches, such as chemical precipitation and osmosis [3]. The most developed microbial remediation techniques are biosorption and biomineralization. Biosorption is constrained by the bioavailability of metal-binding sites [4], however biomineralization mechanisms are less limited. Hence, biomineralization continues to be one of the more promising technologies for metal removal from highly diluted solutions.

The bacterial remediation of uranium in anoxic environments has been previously documented by work mainly focused on the enzymatic reduction of soluble, highly mobile U(VI) to a less toxic, solid U(IV) oxide (uraninite) species [5-8]. Uraninite has low solubility and is very stable in reducing environments. However in oxidizing water, it readily dissolves to form aqueous uranyl complexes [9]. In contrast to anaerobic microbially-induced reductive precipitation, biomineralization takes place under aerobic conditions. Therefore, biomineralization is being considered as a potential remediation strategy for radionuclides in

oxygenated subsurface zones and contaminated ground water [10-12].

Previous studies have described the use of indigenous and genetically introduced recombinant acidic phosphatases for the biomineralization of uranium and its removal from aqueous solutions as uranium phosphate mineral phases [13-15]. However, these studies used an exogenous organic phosphate substrate (e.g. glycerol 2-phosphate) to liberate the inorganic phosphate groups which are responsible for the precipitation of the radionuclide. To date, no study has been performed on the bioprecipitation of U by acid phosphatase from naturally occurring microbes in the absence of an external organic phosphate source. The novelty of this work resides in the fact that the bacterial strains used here are capable of releasing and hydrolyzing stored phosphorus as a consequence of increased cell wall permeability and indigenous acid phosphatase activity.

In this study, we have used U L_{III}-edge X-ray absorption spectroscopy (XAS), TEM/EDX and potentiometric titration to examine the ability of these bacterial strains, isolated from extreme habitats, to bioprecipitate U(VI) from solution under acidic conditions. XAS was used as a suitable tool for the determination of the local coordination of radionuclides in biological systems and for fine atomic characterization of the precipitated amorphous U complexes [16-20].

2. Materials and methods

2.1. Bacteria, isolation media and culture conditions

The two bacterial strains used in this work were isolated from two different extreme habitats. The *Sphingomonas sp*. S15-S1 strain was isolated from a ground water sample; collected at a depth of 290 to 324 meters below the surface from the S15 monitoring well, located near the nuclear waste repository site Tomsk-7 in Siberia, Russia [21]. The *B.*

sphaericus JG-7B strain was isolated from acidic sediment (pH 4.5) of a uranium mining waste pile near the town of Johanngeorgenstadt, Germany [22]. Both strains were isolated using an enrichment culture. An oligotrophic R2A medium was used for the isolation of *Sphingomonas* sp. S15-S1 [23]. In the case of *B. sphaericus* JG-7B, a nutrient broth (NB) medium (8 g L^{-1}, pH 7.0) was employed. Details of the molecular characterization for the isolated species, the acid phosphatase enzymatic assay and colorimetric determination of phosphates are presented in the supporting information.

2.2. Potentiometric titration studies

Potentiometric titrations were carried out to determine the characteristic functional groups present on the bacterial surfaces [24]. All titrations were performed using a Metrohm Titrino 718 STAT automatic titrator (Metrohm, UK) at 25 °C. The temperature was kept constant and continuously monitored during the titration. The titrator was set to only add successive acid or base once a drift equal or less than 5 mV min^{-1} was achieved.

An amount of live bacteria equivalent to 0.05-0.1 g of dry biomass (washed four times with $NaClO_4$) was suspended in a vessel with 25 mL of 0.05, 0.1 or 0.5 M $NaClO_4$, and then purged with N_2 for 1h to remove dissolved CO_2. A positive N_2 gas pressure was maintained during the titration. The suspension was titrated with 0.1 M HCl to pH 3.5 followed by 0.1 M NaOH to pH 10.0. To test the reversibility of the protonation-deprotonation behavior, the suspension was back-titrated with 0.1 M HCl from pH 10.0 to 3.5. The HCl and NaOH were previously calibrated against primary standards.

To calculate the acidity constant (p*K*a) values and the corresponding total concentration of the binding sites for the two strains, *Sphingomonas* sp. S15-S1 and *B. sphaericus* JG-7B, data from five replicates of each titration curve were fitted using the program Protofit 2.1 [25]. Variations in the experimental results are reported as the average ± standard deviation.

2.3. Experimental procedure for XAS sample preparation

Bacterial cells grown to the late-exponential phase were harvested by centrifugation at 15.000 x *g* for 20 min at 4 °C and washed three times with 0.1 M $NaClO_4$ to remove the interfering ingredients of the growth medium. The pellet was suspended in 10 mL of a previously filtered 0.5 mM $UO_2 (NO_3)_2 \cdot 6 H_2O$ solution prepared at three pH values (2.0, 3.0 and 4.5). The samples were shaken for 48 h in an orbital shaker (Gallenkamp, London, UK) at 200 rpm. The cells were harvested by centrifugation after being in contact with the uranium solution and washed with 0.1 M $NaClO_4$. The cell pellets were powdered after being dried in a vacuum incubator at 30 °C for 24 h. Experimental details for the XAS measurements can be found in the supporting information.

2.4. Sample Preparation for TEM/EDX Analyses

Bacterial cells grown to the late-exponential phase were harvested by centrifugation at 15.000 x *g* for 15 min at 4 °C and washed twice using 0.1 M $NaClO_4$ to remove interferences from the growth medium. The pellet was then suspended in 10 mL $UO_2(NO_3)_2$ solution (0.5 mM, pH 2.0, 3.0 and 4.5) and incubated for 48 h. The metal-treated cells were harvested by centrifugation and washed with 0.1 M $NaClO_4$ to remove any excess of uranium solution. The TEM sample preparation was carried out as described in Merroun et al. [17]. The samples were examined using a high-resolution Philips CM 200 transmission electron microscope at an acceleration voltage of 200 kV under standard operating conditions with the liquid nitrogen anti-contaminator in place. Energy-dispersive X-ray (EDX) analysis, which provides elemental information via the analysis of X-ray emissions caused by a high-energy electron

beam, was also performed at 200 kV using a spot size of 70 Å and a live counting time of 200 s.

3. Results

3.1. Phylogenetic affiliation of the bacterial isolates

The phylogenetic affiliation of the two bacterial isolates studied in this work, based on their 16S rRNA gene analysis, is shown in Fig. 1. The results indicated that the strain *B. sphaericus* JG-7B was affiliated with two other strains of *B. sphaericus* (JG-A12 and DSM28) with a 100% of 16S rRNA gene identity. The strain JG-A12 was enriched from a soil sample of the same uranium mining waste pile (near Johanngeorgenstadt, Saxony, Germany) and was demonstrated to have an unusually high capability to bind U(VI) reversibly [17, 26]. The strain DSM28 is the type strain of *B. sphaericus* deposited at the German collection of microorganisms (DSMZ, Braunschweig, Germany). The 16S rRNA gene sequence of the isolate S15-S1 is related to *S. yabuuchiae* A1-18 isolated from the space laboratory Mir [27]. Direct molecular and cultivation dependent approaches have demonstrated that representatives of *Bacillus* and *Sphingomonas* strains, similar to those described here, were also found in extreme habitats including those contaminated with radionuclides and heavy metals. Strains of *Bacillus* species have been recovered from uranium contaminated sites with acidic pH values [26] and high concentrations of inorganic contaminants [16]. Representatives of *Sphingomonas* have also been identified as major components of biofilm populations formed in naturally nickel-rich river water [28]. These bacteria lack special growth requirements and grow easily in nutrient limited environments [29-30].

3.2. Potentiometric Titration studies

The potentiometric titration curves of *Sphingomonas* sp. S15-S1 and *B. sphaericus* JG-7B are presented in Figs. 2A and 2B. The concentration of deprotonated sites is standardized per mass of dry biomass (mol g^{-1}) and calculated according to Fein et al. [31] as follows:

$$[H^+]_{consumed/released} = (C_a - C_b - [H^+] + [OH^-]) / m_b$$

where m_b is the biomass concentration in the suspension (g L^{-1}), C_a and C_b are the concentrations of acid and base added at each step of a titration, and $[H^+]$ and $[OH^-]$ represent molar species concentrations of H^+ or OH^-. In order to calculate the acidity constants and the total concentration of each binding site, the titration curve data was fitted using ProtoFit 2.1 [24] using a Non-Electrostatic Model (NEM).

The titrated bacterial suspensions exhibited a protonation-deprotonation behavior over the whole pH range studied (Figs. 2A and 2B). No evidence of saturation was found with respect to proton adsorption. This indicates that, even at pH 3.5, full protonation of the functional groups on the cell wall was not achieved. For all titration curves, the protonation/deprotonation process was reversible.

Figs. 3A and 3B show a comparison of the titration data at different ionic strengths. An intersection point around pH 5.8 and 5.5 can be seen for *Sphingomonas* sp. S15-S1 and *B. sphaericus* JG-7B, respectively. These values were set as the experimental pH of zero proton charge (pH_{zpc}), and are in agreement to the values predicted by ProtoFit 2.1 (see Table 1). There is an ionic strength effect over the pH range studied (Figs. 3A and 3B). However, these effects are weak when compared to the experimental errors associated with potentiometric titrations of bacteria [31-33].

Table 1 summarizes the p*K*a values for *Sphingomonas* sp. S15-S1 and *B. sphaericus* JG-7B. The calculated values are 4.27 ± 0.45 and 4.37 ± 0.27 for pK_1, 7.03 ± 0.86 and 6.37 ± 0.31

for pK_2 and 9.92 ± 0.32 and 9.95 ± 0.16 for pK_3, for *Sphingomonas* sp. S15-S1 and *B. sphaericus* JG-7B respectively. The obtained p*K*a values are representative of carboxylic groups for pK_1, phosphate groups for pK_2 and amine and hydroxyl groups for pK_3 [34-36].

The surface site densities obtained using ProtoFit are also presented in Table 1. The p*K*a values for both bacterial strains are comparable indicating similar concentration of the active functional groups on the cell wall. However, the concentration corresponding to amine/hydroxyl groups (C_3) is slightly higher for *Sphingomonas* sp. S15-S1.

3.3. X-ray Absorption spectroscopy

A visual comparison of the XANES fingerprints for the reference samples U(VI) and U(IV) indicated the presence of U(VI) in the six samples studied in this work (Figs. 4A and 4B). The presence of U(VI) in the XANES spectra is evidenced by the display of a characteristic shoulder at 17.188 eV, which is consistent with the U(VI) oxidation state [37].

The uranium L_{III}-edge EXAFS spectra and their corresponding Fourier transforms (FT) for the uranium species formed at pH 2.0, 3.0 and 4.5 by the cells of *Sphingomonas* sp. S15-S1 and *B. sphaericus* JG-7B are presented in Figs. 5A and 5B. The FT represents a pseudo-radial distribution function of the uranium near-neighbor environment.

The FT of the EXAFS spectra of the samples at pH 2.0, 3.0 and 4.5 show five to six significant peaks (Figs. 5A and B). Tables 2 and 3 show the quantitative fit results (distances are phase shift corrected). The adsorbed U(VI) observed has the common linear trans-dioxo structure: two axial oxygen atoms at a radial distance of 1.76 - 1.79 ± 0.02 Å, and an equatorial shell of 4 to 5 oxygen atoms at 2.27 - 2.36 ± 0.02 Å. As evident from the results presented in Tables 2 and 3, the coordination numbers, bond distances and Debye-Waller factors of the U-O_{eq1} shell are affected by the pH of the uranium solution. A four-fold coordination of uranium to ligands of the bacterial cells (N ~ 4 and R= 2.27 ± 0.02 Å) was

observed on the EXAFS spectra of both bacterial strains at pH 4.5 and in that of the JG-7B at pH 3. The lower Debye-Waller factors obtained (0.0040-0.0046 $Å^2$), indicated the absence of a disorder in U-O_{eq1} distances contributing to the EXAFS signal. However, the higher Debye-Waller factor of the EXAFS spectrum of S15-S1 at pH 3 (0.0132 $Å^2$) indicated that there is probably a wide spread of U-O_{eq1} distances with an average value of 2.32 ± 0.02 Å. The samples incubated at pH 2.0, showed the presence of a five-fold uranium coordination (N ~ 5 and R= 2.34-2.36 ± 0.02 Å). The U-O_{eq1} bond distance is within the range of previously reported values for phosphate bound to uranyl [16-21].

Adding an oxygen shell at a distance of R = 2.82-2.87 ± 0.02 Å improved significantly the fit for all samples. The fitted distance between uranium and oxygen atoms is not related to direct bonding but has been previously interpreted as scattering contributions from neighboring ligand shells known as "short contacts" in crystallography [16,21].

The fifth FT peak observed at R+Δ ~ 3 Å (radial distance R = 3.59 - 3.62 Å), is the result of a back-scattering from phosphorus atoms. This distance is typical for a mono-dentate coordination of U(VI) by phosphate [16-21].

The EXAFS spectra of the U-treated bacterial cell samples at pH 4.5 and that of JG-7B treated at pH 3.0 are comparable to the spectra of meta-autunite. All spectra showed similar features and distances for U-O_{eq}, U-P and U-U. These findings suggest the precipitation of an inorganic m-autunite-like uranyl phosphate by the bacterial cells.

The EXAFS spectra of the samples treated at pH 2.0 showed close similarities to that of organic phosphate ligands complexed with U such as fructose 1,6-phosphate (see Fig. 5) [38]. At pH 3, the EXAFS spectrum of S15-S1 may consist of both uranyl phases (organic and inorganic phosphates complexes). This suggestion is supported by the high Debye-Waller factor value of the U-O_{eq1} bond distance (Table 3).

3.4. Cellular localization of the bound U(VI) by TEM

The TEM of *B. sphaericus* JG-7B cells exposed to U solution (0.5 mM, pH 4.5) (Fig. 6A) revealed the presence of electron-dense accumulations on the cell surface. There was no intracellular accumulation of U observed in these samples. The EDX spectrum derived from these deposits (Fig. 6B) indicated that their chemical composition was mainly oxygen (O), phosphorus (P), and uranium (U). In the case of *Sphingomonas* sp. S15-S1, samples prepared at pH 2.0 showed very small amount of U bound to bacterial cell surfaces of both isolates (data not shown). Similarly to *B sphaericus*, the presence of U associated with intracellular space was not observed. At pH 3.0 and 4.5, *Sphingomonas* sp. S15-S1 cells accumulated U in the form of precipitates at the cell membrane and intracellular accumulation of U was also observed in the form of electron dense granules (Figs. 7A-E). EDX analysis of the intracellular and cell wall deposits of the thin sections of the Figs. 7A-B shown in Figs. 7F-G, respectively, indicated the presence of phosphorus and U.

3.5. Acidic phosphatase activity and determination of inorganic phosphate

The measured acidic phosphatase (APase) activity of JG-7B and S15-S1 cell suspension at pH 2.0, 3.0 and 4.5 are presented in Fig. 8. In addition, the APase activity was also calculated for heat-killed cells.

The results indicate that the enzymatic activity is highly strain-specific. The cells of the strain S15-S1 showed activities 20 orders of magnitude higher than those of the strain JG-7B. In both cases, the phosphatase activity increases with increasing pH and reaches an optimum value at pH 4.5. Acidic phosphatase activity (within the experimental errors) was neither detected in the suspensions of heat-killed cells, nor in cells incubated in $NaClO_4$ at pH 2.0 for both strains.

The concentration of orthophosphate in the supernatants of the cells of the two strains incubated for 48 h at pH 4.5 in 0.1 M $NaClO_4$ (control sample) and in 0.5 mM uranium solution (U treated samples) are shown in Fig. 9. As evident from this figure, the amount of the orthophosphate liberated by the control samples is two to three orders of magnitude higher than the samples containing U.

4. Discussion

In the present work, a complex methodological approach involving a combination of surface chemistry, transmission electron microscopy and advanced solid state speciation techniques were used to characterize uranium biomineralization mechanisms. Bacterial strains isolated from two different extreme environments were studied under acidic and aerobic conditions. The studied strains were: the Gram-positive strain *B. sphaericus* JG-7B, cultivated from a uranium mining waste sediment in Germany; and the Gram-negative Alphaproteobacterial strain *Sphingomonas* sp. S15-S1, recovered from ground water extracted from the S15 deep monitoring well of the Siberian radioactive waste subsurface depository Tomsk-7 in Russia. In these extreme environments, bacteria may interact efficiently with these inorganic contaminants through different mechanisms such as intracellular accumulation [16], precipitation [39,40] and biosorption at the cell surfaces [17].

4.1. *Potentiometric Titration studies*

Bacterial cell walls contain a variety of functional groups that provide metal binding sites, such as hydroxyl, phosphoryl, amino, and carboxylate groups. These functional groups can protonate or deprotonate when interacting with their immediate surroundings and as a result the cell walls develop a net pH-dependent charge [24,32,34,41-42]. Therefore, knowledge of

the cell surface properties is crucial to understand the interaction mechanisms between bacteria and surrounding metals. The concentration and characteristics of proton active carboxylic, hydroxyl, phosphate, phosphodiester, and amine groups on the cell surfaces play an important role in this respect, as they are responsible for surface binding ability [36]. The results of potentiometric titration experiments on the studied *Sphingomonas* sp. and *B. sphaericus* strains indicated that the cell surface groups capable for metal binding are sites involving carboxyl groups (pK < 4.27-4.37), sites involving phosphate groups (pK ≈ 7), and sites involving hydroxyl and amine groups (pK > 8). These findings are in agreement with previous studies on bacterial surfaces [31, 42]. Haas et al. [42] showed that in the presence of U(VI), sorption is accounted for by using two separate adsorption reactions that form the surface complexes >COO–UO_2^+ and >PO_4H–$UO_2(OH)_2$. This mechanism indicates that phosphate and carboxyl groups are expected to be involved in the binding of this radionuclide. However, XAS studies demonstrated that for the investigated bacterial strains, phosphate groups are the main binding sites for uranium in the pH range studied. The extent of the carboxyl group involvement in the uranium binding is probably too insignificant to be detected by titration methods.

The titration studies also showed that the surface site density of *B. sphaericus* JG-7B is similar to those found for *B. subtilis* by Chatellier and Fortin [43], except for the lower value obtained for phosphate groups on *B. sphaericus*. Cox et al. [44] reported that the presence of a thick peptidoglycan layer on Gram positive bacteria seems to be responsible for a higher binding capacity for metals. The *Sphingomonas* sp. and *B. sphaericus* JG-7B strains studied in this work showed site densities of the same order of magnitude, suggesting a similar potential capacity to bind metals.

4.2. X-ray Absorption spectroscopy molecular scale analysis of U/bacteria complexes

The speciation of U associated with cells under the studied conditions is a pH dependent process. At pH 4.5, EXAFS analysis indicated that cells of the S15-S1 and JG-7B strains precipitated uranium as a meta-autunite mineral-like phase since the local coordination of U in these samples matches that of meta-autunite. In addition, evidence from the acidic phosphatase studies indicated the presence of phosphatase enzyme in the cell suspensions. These findings suggest a direct link on the precipitation of U by liberation of inorganic phosphates in solution. The amount of the orthophosphate in the supernatant of U treated samples of S15-S1 and JG-7B decreased by 2 to 3 orders of magnitude in comparison to that of the control sample, indicating that these ions are scavenged for the precipitation of U in solution. The implication of acid phosphatase activity in the precipitation of U is supported by the fact that at pH 2 no enzymatic activity was detected and therefore uranium biomineralization did not occur. Several studies reported the role played by this enzyme in the liberation of inorganic phosphates that precipitate uranium [16,39,45,46]. *Citrobacter* sp. was shown to accumulate heavy deposits of uranyl phosphate at the cell surface after enzymatically liberating phosphate ligands *via* the activity of a phosphatase, resulting in biomineralization of $NaUO_2PO_4$ and/or HUO_2PO_4 [46]. Indigenous acidic phosphatase activity in naturally occurring strains of the genera *Bacillus* and *Rahnella* isolated from radionuclide- and metal-contaminated soils has been recently demonstrated to be involved in the precipitation of uranium [15]. This is due to the liberation of orthophosphate from the added glycerol-3-phosphate as a source of organic phosphates.

In the present study, no organic phosphate sources were added to the metal-bacteria mixture. At this stage of investigation, the origin of the phosphates which precipitate U is still unknown. One possible source of organic phosphate is the lysis of dead cells. The presence of dead cells in the treated samples was demonstrated earlier in our previous study by using TEM [21]. In the same work we have shown also by using live/dead staining approach that the percentage of dead cells represents 40% of the cell population. In uranium contaminated

sites, dead cells of U-sensitive microbial populations will liberate significant quantities of biopolymers able to precipitate uranium after lysis [47-48]. These phosphorylated biological components could be used as substrates for acidic phosphatase activity, precipitating uranium. Similar results were found with microbial strains *Myxococcus xanthus* [39] and *Sulfolobus acidiocaldarius* [49] which precipitated uranium as an m-autunite-like phase due to the activity of indigenous acidic phosphatase expressed in uranium treated cell suspensions without an external organic phosphate source. The biomineralization of uranium by bacteria based on indigenous or introduced recombinant alkaline phosphatase has been proposed as appropriate technology for the treatment of alkaline waters containing uranium [50].

At pH 3, the speciation of U associated with cells of the two strains is dominated by the uranium phosphate mineral phase. Uranium organic phosphate species were found on samples of JG-7B cells. In the case of strain S15-S, the uranium speciation is a mixture of U organic phosphate species and U inorganic phosphates mineral phases. The mixture of these two U phases is evidenced by the high Debye-Waller factor of the U-O_{eq1} shell, estimated to be 0.0132 $Å^2$ by EXAFS spectroscopy.

4.3. TEM cellular localization of U precipitates

The presence of precipitated uranium at cell level is strain-specific and affected by the uranium solution pH as demonstrated by TEM analysis. *B. sphaericus* JG-7B cells precipitated uranium at the cell wall, which consists of peptidoglycan and S-layer protein. The latter envelope component may play a crucial role in the protection of the cells of this bacterium against uranium toxicity. These results are in agreement with those found for a different *B. sphaericus* strain, where the accumulated uranium was only localized at the cell envelope [16]. In the case of *Sphingomonas* sp., microscopic observations of cells exposed to uranium solution showed electron-dense precipitates at the cell envelope and in some cases

also within the cells. The intracellular accumulation occurs in two different forms, as electron dense granules and as needle-like fibrils. These findings reveal that Gram-negative and Gram–positive bacteria accumulate uranium via different mechanisms. These differences could be explained by variations on the structural composition of their cell walls.

4.4 Environmental implication of U biomineralization at acidic conditions

The remediation of polluted sites by conventional methods, such as excavation and pump and treat, can be costly and disruptive. Therefore *in situ* remediation strategies, based on the stimulation of the growth of microbial strains with acid phosphatase activity such as the ones reported here (*Sphingomonas* sp. and *Bacillus* sp.), could be considered as a potential strategy for decontamination of such environments. The high acid phosphatase activity demonstrated for these strains makes them ideal candidates to use on bioremediation of uranium contaminated sites. The natural habitats of these bacteria are characterized by extremely complex biogeochemistry (low pH values, high concentrations of heavy metals) and high microbial diversity and activity. Despite these complexities, these bacterial strains are capable to produce inorganic phosphate species in sufficient quantities to remove at least 70% (and in some cases nearly 100%) of U(VI) from solution via phosphate-associated precipitates. These characteristics add extra features to the biomineralization process widening the possibilities of using this technique as a remediation route for radionuclides in the environment.

5. Conclusions

This study demonstrates that inorganic phosphate responsible for uranium biomineralization at pH 4.5 and 3 is liberated by the cells of *Sphingomonas* sp. and *B. sphaericus* strains, as a consequence of both increased cell wall permeability and the APase

activity of the strains. The impact of uranium precipitation at acidic and aerobic conditions by bacteria isolated from different extreme environments must be acknowledged in attempts to fully understand actinide cycling and dispersal in the environment. This work supports previous findings that uranium bioremediation could be achieved via the biomineralization of U(VI) in phosphate minerals as a complementary process to the more widely investigated U(VI) bioreduction.

Acknowledgments

This work was supported partly by grant FIKW-CT-2000-00105 (BORIS) from the European Community and also from the Grant No CGL2009-09760 and CGL2007-61489 from the Ministerio de Ciencia e Innovación, and Ministerio de Educación y Ciencia, respectively, Spain. We thank A. Scheinost and H. Funke from ROBL, ESRF, Grenoble for their help in the EXAFS measurements. J. J. Ojeda acknowledges funding from the UK Engineering and Physical Sciences Research Council (EPSRC), as part of the DIAMOND Consortium: Decommissioning, Immobilisation and Management of Nuclear wastes for Disposal (EP/F055412/1).

References

[1] M. Fomina, J.M. Charnock, S. Hillier, R. Alvarez, G.M. Gadd, Fungal transformations of uranium oxides, Environ. Microbiol. 9 (2007) 1696-1710.

[2] M. Beleites, Altlast Wismut. Brandes and Apsel, Frankfurt am Main, 1992.

[3] H. Brim, S.C. McFarlan, J.K. Fredrickson, K.W. Minton, M. Zhai, L.P. Wackett, M.J. Daly, Engineering *Deinococcus radiodurans* for metal remediation in radioactive mixed waste environments, Nat. Biotechnol. 18 (2000) 85-90.

[4] L.E. Macaskie, An immobilized cell bioprocess for the removal of heavy metals from aqueous flows, J. Chem. Technol. Biotechnol. 49 (1990) 357-379.

[5] J.D. Wall, L.R. Krumholz, Uranium reduction, Annu. Rev. Microbiol. 60 (2006) 149-166.

[6] D.R. Lovley, E.J.P. Phillips, Y.A. Gorby, E.R. Landa, Microbial reduction of uranium. Nature 350 (1991) 413–416.

[7] Y. Suzuki, T. Suko, Geomicrobiological factors that control uranium mobility in the environment: Update on recent advances in the bioremediation of uranium-contaminated sites. J. Mineral. Petrol. Sci. 101 (2006) 299–307.

[8] J.R. Lloyd, J. Chesnes, S. Glasauer, D.J. Bunker, F.R. Livens, D.R. Lovely, (2002) Reduction of actinides and fission products by Fe(III)-reducing bacteria, Geomicrobiol. J. 19 (2002) 103-120.

[9] D. Langmuir, Uranium solution-mineral equilibria at low temperatures with applications to sedimentary ore deposits, Geochim. Cosmochim. Acta 42 (1978) 547-569.

[10] N. Renninger, R. Knopp, H. Nitsche, D. Clark, J. Keasling, Uranyl precipitation by *Pseudomonas aeruginosa* via controlled polyphosphate metabolism, Appl Environ. Microbiol 70 (2004) 7404-7412.

[11] E.S. Shelobolina, H. Konishi, H. Xu, E.E. Roden, U(VI) Sequestration in

hydroxyapatite produced by microbial glycerol 3-phosphate metabolism, Appl. Environ. Microb.75 (2009) 5773-5778.

[12] S. Choudhary, P. Sar, Uranium biomineralization by a metal resistant Pseudomonas aeruginosa strain isolated from contaminated mine waste, J. Hazard Mater.186 (2011) 336-343.

[13] L.E. Macaskie, R.M. Empson, A.K. Cheetham, C.P. Grey, A.J. Skarnulis, Uranium bioaccumulation by a *Citrobacter* sp. as a result of enzymically mediated growth of polycrystalline HUO_2PO_4, Science 257 (1992) 782-784.

[14] P. Yong, L.E. Macaskie, Role of citrate as complexing ligand which permits enzymatically-mediated uranyl ion bioaccumulation, Bull. Environ. Contam. Toxicol. 54 (1995) 892-899.

[15] R.J.M. Martinez, J. Beazley, M. Teillefert, A.K. Arakaki, J. Skolnick, P.A. Sobecky, Aerobic uranium (VI) bioprecipitation by metal-resistant bacteria isolated from radionuclide- and metal-contaminated subsurface soils, Environ. Microbiol. 9 (2007) 3122-3133.

[16] M.L. Merroun, C. Hennig, A. Rossberg, T. Reich, S. Selenska-Pobell, Characterization of U(VI)-*Acidithiobacillus ferroxidans* complexes using EXAFS, transmission electron microscopy and energy-dispersive X-ray analysis, Radiochim. Acta 91 (2003) 583-591.

[17] M.L. Merroun, J. Raff, A. Rossberg, C. Hennig, T. Reich, S. Selenska-Pobell, Complexation of uranium by cells and S-layer sheets of *Bacillus sphaericus* JG-A12, Appl. Environ. Microbiol. 71 (2005) 5532-5543.

[18] M.L. Merroun, M. Nedelkova, A. Rossberg, C. Hennig, S. Selenska-Pobell, Interaction mechanisms of bacterial strains isolated from extreme habitats with uranium, Radiochim. Acta 94 (2006) 723-729.

[19] M.L. Merroun, S. Selenska-Pobell, Bacterial interactions with uranium: and

environmental perspective, J. Contam. Hydrol. 102 (2008) 285-295.

[20] M. Neu, H. Boukhalfa, M.L. Merroun, Biomineralization and biotransformations of actinide materials. MRS Bulletin 35 (2010) 849-857.

[21] M. Nedelkova, Microbial diversity in ground water at the deep-well monitoring site S15 of the radioactive waste depository Tomsk-7, Siberia, Russia. PhD thesis. University of Freiberg, Freiberg, Germany, 2005.

[22] K. Brottka, Diploma thesis, Technical University of Dresden, Germany, 2003.

[23] D.J. Reasoner, E. Geldreich, A new medium for the enumeration and subculture of bacteria from potable water, Appl. Environ. Microbiol. 49 (1985) 1-7.

[24] J.B. Fein, J. Boily, N. Yee, D. Gorman-Lewis, B.F. Turner, Potentiometric titrations of *Bacillus subtilis* cells to low pH and a comparison of modelling approaches, Geochim. Cosmochim. Acta 69 (2005) 1123-1132.

[25] B.F. Turner, J.B. Fein, Protofit: A program for determining surface protonation constants from titration data, Comput. Geosci-UK. 32 (2006) 1344-1356.

[26] S. Selenska-Pobell, V. Miteva, I. Boudakov, P. Panak, G. Bernhard G, H. Nitsche, Selective accumulation of heavy metals by three indigenous *Bacillus* isolates, *B. cereus, B. megaterium and B. sphaericus* in drain waters from a uranium waste pile, FEMS Microbiol. Ecol 29 (1999) 59-67.

[27] Y. Li, Y. Kawamura, N.T. Fujiwara, H. Liu, X. Huang, K. Kobayashi, T. Ezaki, *Sphingomonas yabuuchiae* sp. nov. and *Brevundimonas nasdae* sp. nov., isolated from the Russian space laboratory Mir. Int. J. Syst. Evol. Microbiol. 54 (2004) 819-825.

[28] J.R. Lawrence, M.R. Chenier, R. Roy, D. Beaumier, N. Fortin, G.D.W. Swehorne, T.R. Neu, C.W. Greer, Microscale and molecular assessment of impacts of nickel, nutrients and oxygen level on structure and function of river biofilm communities, Appl. Environ. Microbiol. 70 (2004) 4326-4339.

[29] D.L. Balkwill, J.K. Fredrickson, M.F. Romine, *Sphingomonas* and related genera. in

M. Dworkin and others (eds.), The Prokaryotes and evolving electronic resource for the Microbiological community, Springer, New York, 2003.

[30] D.C. White, S. Sutton, D. Ringelberg, The genus *Sphingomonas* physiology and ecology, Curr. Opin. Biotechnol. 7 (1995) 301-306

[31] J.B. Fein, C.J. Daughney, N. Yee, T.A. Davis, A chemical equilibrium model for metal adsorption onto bacterial surfaces, Geochim. Cosmochim. Acta 61 (1997) 3319-3328.

[32] C.J. Daughney, J.B. Fein, Effect of ionic strength on the adsorption of H^+, Cd^{2+}, Pb^{2+}, and Cu^{2+} by *Bacillus subtilis* and *Bacillus licheniformis*: A surface complexation model, J. Colloid Interface Sci. 198 (1998) 53-77.

[33] R.E. Martinez, D.S. Smith, E. Kulczycki, F.G. Ferris, Determination of intrinsic bacterial surface acidity constants using a Donnan shell model and a continuous pK_a distribution method, J. Colloid Interface Sci. 253 (2002) 130-139.

[34] B. Ngwenya, I. Sutherland, L. Kennedy, Comparison of the acid-base behaviour and metal adsorption characteristics of a gram-negative bacterium with other strains, Appl. Geochem. 18 (2003) 527-538.

[35] N. Yee, L.G. Benning, V.R. Phoenix, F.G. Ferris, Characterization of metal-cyanobacteria sorption reactions: a combined macroscopic and infrared spectroscopic investigation, Environ. Sci. Technol. 38 (2004) 775-782.

[36] M. Dittrich, S. Silber, Cell surface groups of two picocyanobacteria strains studied by zeta potential investigations, potentiometric titration, and infrared spectroscopy, J. Colloid Interface Sci. 286 (2005) 487-495.

[37] E. Hudson, A.P.G. Allen, L.J. Terminello, Polarized X-ray absorption spectroscopy of the uranyl ion: Comparison of experiment and theory, Phys. Rev. B 54 (1996) 156-165.

[38] A. Koban, G. Geipel, A. Roßberg, G. Bernhard, (2004) Uranyl (VI) complexes with sugar phosphates in aqueous solution, Radiochim. Acta 92 (2004) 903-908.

[39] F. Jroundi, M.L. Merroun, J.M. Arias, A. Rossberg, S. Selenska-Pobell, M.T. González-Muñoz, Spectroscopic and microscopic characterization of uranium biomineralization in *Myxococcus xanthus*, Geomicrobiol. J. 24 (2007) 441-449.

[40] M. Nedelkova, M.L. Merroun, A. Rossberg, C. Hennig, S. Selenska-Pobell, (2007) *Microbacterium* isolates from the vicinity of a radioactive waste depository and their interactions with uranium, FEMS Microbiol. Ecol. 59 (2007) 694-705.

[41] A.C.C. Plette, W.H. van Riemsdijk, M.F. Benedetti, A. van de Wal, pH dependent charging behaviour of isolated cell walls of a gram-positive soil bacterium, J. Colloid Interface Sci. 173 (1995) 354-363.

[42] J.R. Haas, T.J. Dichristina, R. Wade, Thermodynamics of U(VI) sorption onto *Shewanella putrefaciens*, Chem. Geol. 180 (2001) 33-54.

[43] X. Chatellier, D. Fortin, Adsorption of ferrous ions onto *Bacillus subtilis* cells, Chem. Geol. 212 (2004) 209–228.

[44] J.S. Cox, D.S. Smith, L.A. Warren, F.G. Ferris, Characterizing heterogeneous bacterial surface functional groups using discrete affinity spectra for proton binding, Environ. Sci. Technol. 33 (1999) 4514-4521.

[45] M.J. Beazley, R.J. Martinez, P.A. Sobecky, S.M. Webb, M. Taillefert, Uranium biomineralization as a result of bacterial phosphatase activity: Insight from bacterial isolates from a contaminated subsurface, Environ. Sci. Technol. 41 (2007) 5701-5707.

[46] L.E. Macaskie, K.M. Bonthrone, P. Yong, D.T. Goddard, Enzymically mediated bioprecipitation of uranium by a *Citrobacter* sp. A concerted role for exocellular lipopolysaccharide and associated phosphatase in biomineral formation, Microbiology 146 (2000) 1855-1867.

[47] B.E. Kalinowski, A. Oskarsson, Y. Albinsson Y, J. Arlinger, A. Ödegaard-Jensen, T. Andlid, K. Pedersen, Microbial leaching of uranium and other trace elements from shale nine tailings at Ranstad, Geoderma 122 (2004) 177-194.

[48] R. Rosen, D. Becher, K. Büttner, D. Biran, A. Hecker, E.Z. Ron, (2004) Highly phosphorylated bacterial proteins, Proteomics 4 (2004) 3068-3077.

[49] T. Reitz, M.L. Merroun, A. Rossberg, R. Steudner, S. Selenska-Pobell, Bioaccumulation of U(VI) by *Sulfolobus acidocaldarius* at moderate acidic conditions, Radiochim. Acta (in press).

[50] K.S. Nilgiriwala, A. Alahari, A.S. Rao, S.K. Apte1, Cloning and overexpression of alkaline phosphatase PhoK from *Sphingomonas* sp. strain BSAR-1 for bioprecipitation of uranium from alkaline solutions, Appl. Environ. Microbiol. 74 (2008) 5516-5523.

FIGURES LEGEND

Fig. 1. 16S rDNA based affiliation of the studied bacterial isolates (given in bold), recovered from extreme environments.

Fig. 2. Potentiometric titration data for cell suspensions of *Sphingomonas* sp. S15-S1 (A) and *B. sphaericus* JG-7B (B) compared with the 0.1M $NaClO_4$ electrolyte. Closed symbols correspond to the forward titration data and open symbols correspond to back titration.

Fig. 3. Potentiometric titration data for cell suspensions of *Sphingomonas* sp. S15-S1 (A) and *B. sphaericus* JG-7B (B) at different electrolyte concentrations (0.05, 0.1 and 0.5M $NaClO_4$).

Fig. 4. Normalized uranium L_{III}-edge XANES spectra of 0.04 M U(IV) in 1 M $HClO_4$, 0.04 M U(VI) in 1 M $HClO_4$, U(VI)-treated cells of JG-7B and S15-S1 isolates at pH 2, 3 and 4.5. The spectra were normalized to equal intensity at 17230 eV.

Fig. 5. Uranium L_{III}-edge k^3–weighted EXAFS spectra (left) and the corresponding Fourier transforms (FT) (right) of uranium complexes formed by the cells of bacterial isolates at pH values 2, 3 (A) and 4.5 (B) and reference compounds (m-autunite and U-fructose(1,6) phosphate).

Fig. 6. Transmission electron micrographs (A), coupled with Energy Dispersive X-ray spectrum (B), of a thin section of *B. sphaericus* JG-7B treated with uranium at pH 4.5. The metal accumulated is localized on the cell surface.

Fig. 7. Transmission electron micrographs of thin sections of *Sphingomonas* sp. S15-S1 treated with uranium at pH 4.5 (A, B) and 3 (C, D, E). Energy Dispersive X-ray spectra of intracellular (F) and cell wall (G) U precipitates showed by heads of B and D, respectively.

Fig. 8. Acidic phosphatase activity of cells of *Sphingomonas* sp. S15-S1 and *B. sphaericus* JG-7B incubated in 0.1 M $NaClO_4$ for 48 h at pH 2, 3 and 4.5, and that of heat killed cells.

Fig.9. Concentrations of ortho-phosphates liberated in the supernatant by cells of *Sphingomonas* sp. S15-S1 and *B. sphaericus* JG-7B -incubated in 0.1 M $NaClO_4$ (control sample) and -treated with 0.5 mM U at pH 4.5.

Table(s)

Table 1: Deprotonation constants and surface site concentrations for *Sphingomonas* sp. S15-S1 and *B. sphaericus* JG-7B as calculated by ProtoFit 2.1

	pK_1	pK_2	pK_3	C_1 ($x10^{-4}$ mol/g)	C_2 ($x10^{-4}$ mol/g)	C_3 ($x10^{-4}$ mol/g)	pH_{zpc}
Sphingomonas sp. S15-S1	4.27±0.45	7.03±0.86	9.92±0.32	4.91±1.04	3.16±0.56	9.24±2.97	5.75±0.54
B. sphaericus JG-7B	4.37±0.27	6.37±0.31	9.95±0.16	4.70±0.55	2.19±0.25	4.56±0.77	5.55±0.28

Table(s)

Table 2. Structural parameters of the uranium complexes formed by the bacterial isolates at pH 2 and 3

Sample	Shell	N[a]	R(Å)[b]	σ^2 (Å^2)[c]	ΔE (eV)
					-12.40
JG-7B pH2	U-O_{ax}	2[d]	1.77	0.0024	
	U-O_{eq1}	4.4(4)	2.36	0.0071	
	U- O_{eq2}	0.8(2)	2.86	0.0038[d]	
	U-P	2.6(4)	3.62	0.0027	
	U- O_{eq1}-P (MS)	5.2	3.74	0.0027	
JG-7B pH 3	U-O_{ax}	2[d]	1.79	0.0024	-12.60
	U-O_{eq1}	4.2(3)	2.27	0.0052	
	U- O_{eq2}	1.0(2)	2.87	0.0038[d]	
	U-P	3.2(5)	3.60	0.0040	
	U- O_{eq1}-P (MS)	6.4	3.72	0.0040	
	U-U	3.2(6)	5.21	0.0080[d]	
S15-S1 pH 2	U-O_{ax}	2[d]	1.77	0.0025	-13.40
	U-O_{eq1}	4.8(5)	2.34	0.0105	
	U- O_{eq2}	0.8(2)	2.86	0.0038[d]	
	U-P	1.5(3)	3.60	0.0010	
	U- O_{eq1}-P (MS)	3.0	3.73	0.0010	
S15-S1 pH 3	U-O_{ax}	2[d]	1.76	0.0040	-15.50
	U-O_{eq1}	4.6(6)	2.32	0.0132	
	U- O_{eq2}	0.7(3)	2.82	0.0038[d]	
	U-P	1.9(5)	3.59	0.0034	
	U- O_{eq1}-P (MS)	3.8	3.72	0.0034	

a: Errors in coordination numbers are ±25%, and standard deviations, as estimated by EXAFSPAK are given in parentheses.
b: errors in distance are ±0.02 Å.
c: Debye-Waller factor.
d: value fixed for calculation.

Table(s)

Table 3. Structural parameters of the uranium complexes formed by the bacterial isolates at pH 4.5

Sample	Shell	N[a]	R(Å)[b]	σ^2 (Å^2)[c]	ΔE (eV)
S15-S1	U-O_{ax}	2[d]	1.77	0.0021	-13.54
	U-O_{eq1}	4.0(3)	2.27	0.0082	
	U- O_{eq2}	0.8(1)	2.86	0.0038[d]	
	U-P	1.8(2)	3.59	0.0040[d]	
	U- O_{eq1}-P (MS)	3.6	3.71	0.0040[d]	
	U-U	1.9(6)	5.19	0.0080[d]	
JG-7B	U-O_{ax}	2[d]	1.79	0.0024	-12.40
	U-O_{eq1}	4.4(2)	2.27	0.0046	
	U- O_{eq2}	1.0(2)	2.85	0.0038[d]	
	U-P	3.2(5)	3.61	0.0050	
	U- O_{eq1}-P (MS)	6.4	3.72	0.0050	
	U-U	2.4(6)	5.20	0.0080[d]	

a: Errors in coordination numbers are ±25%, and standard deviations, as estimated by EXAFSPAK are given in parentheses.
b: errors in distance are ± 0.02 Å.
c: Debye-Waller factor.
d: value fixed for calculation.

Figure(s)

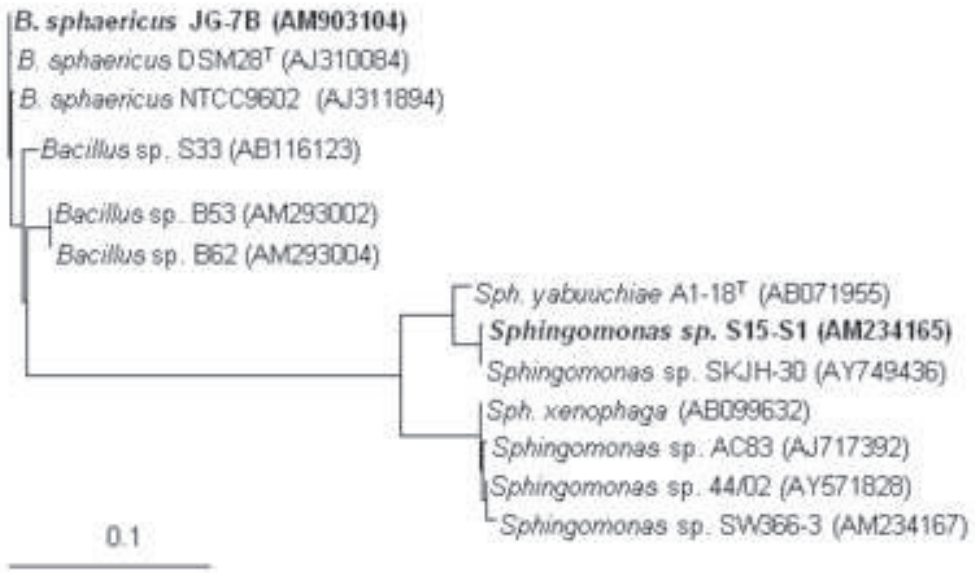

FIG. 1

Figure(s)

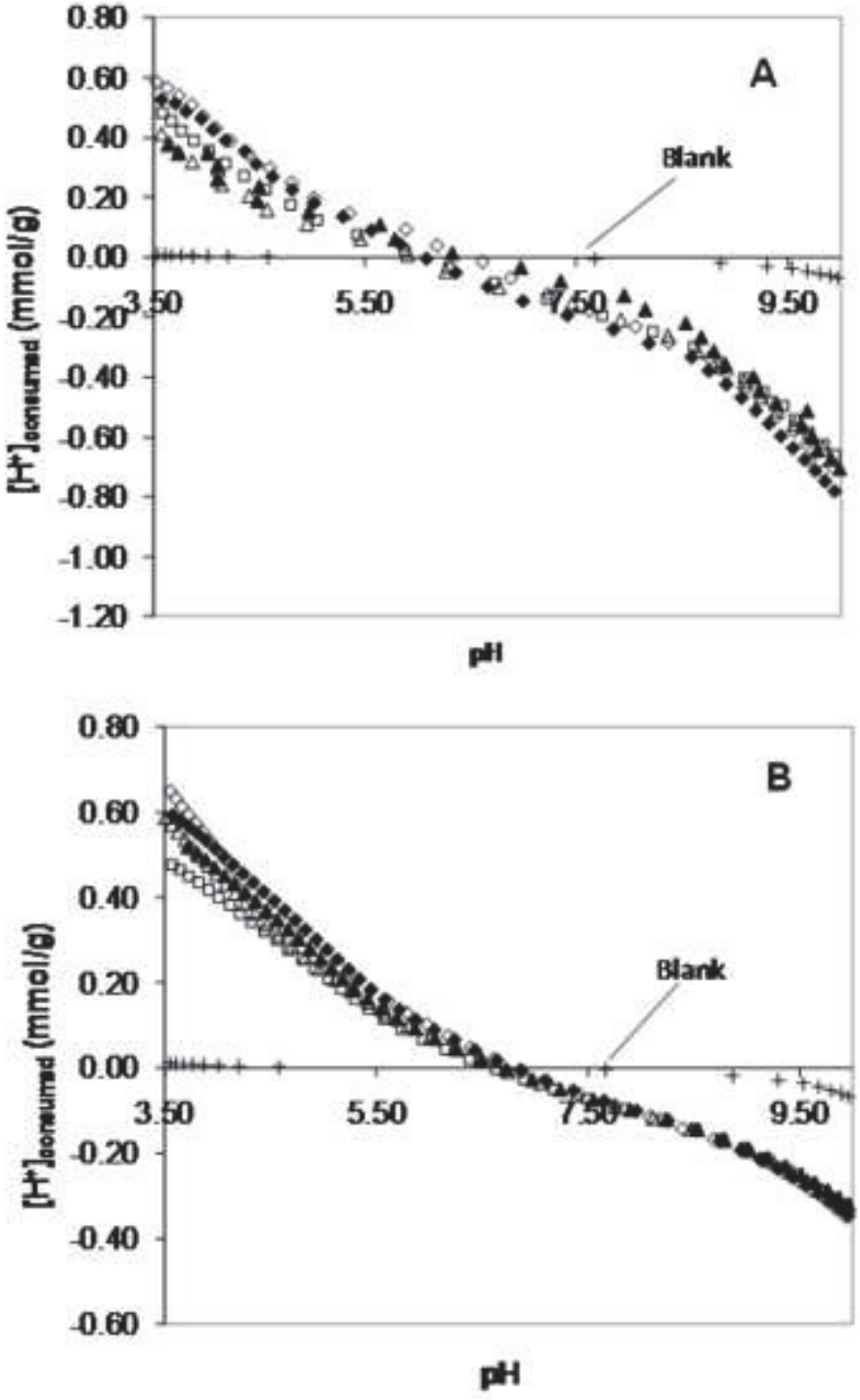

FIG. 2

Figure(s)

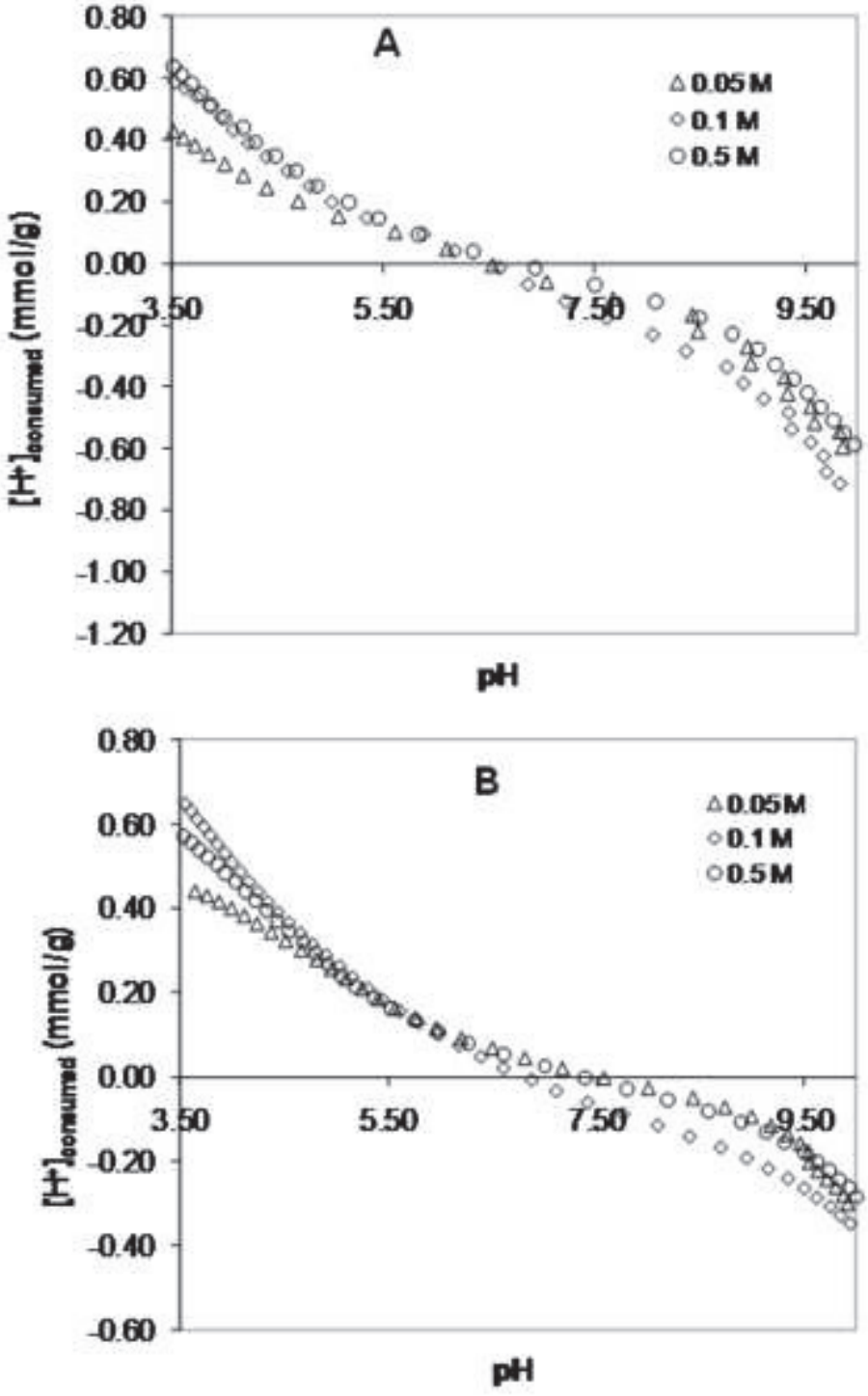

FIG. 3

Figure(s)

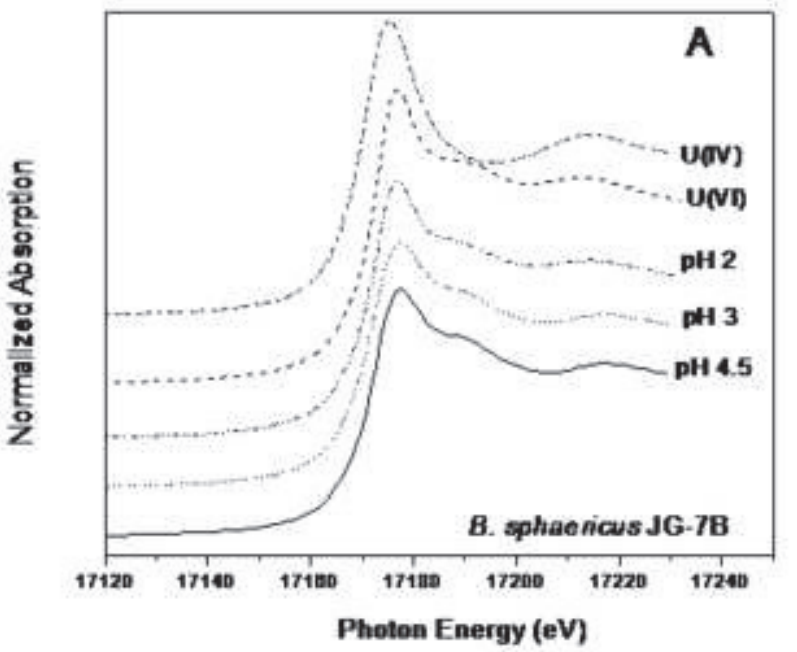

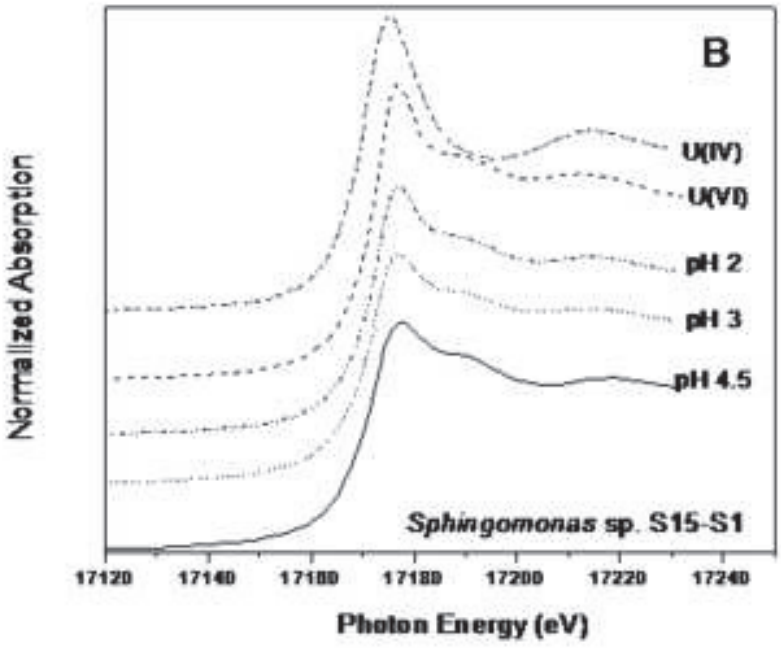

FIG. 4

Figure(s)

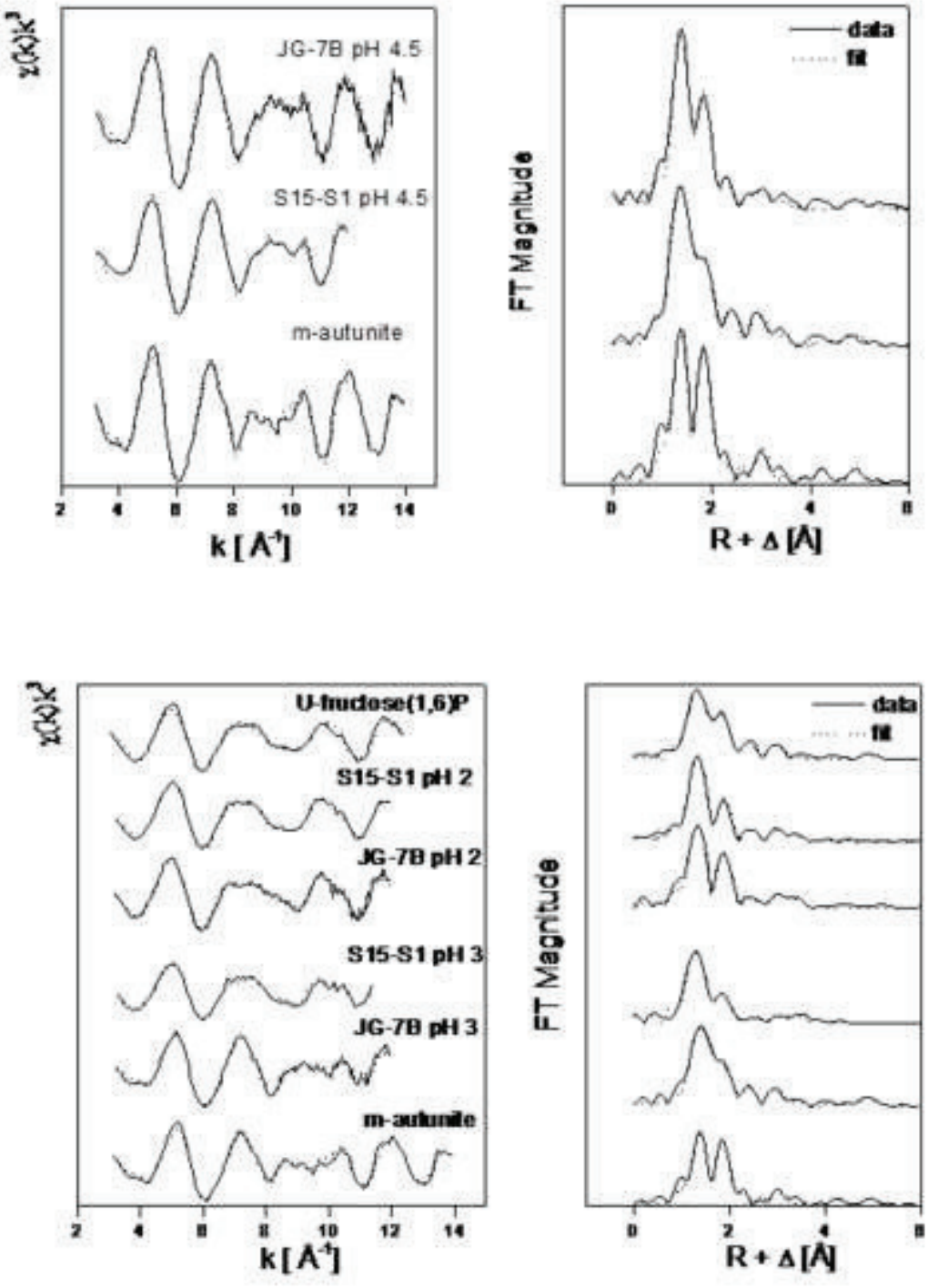

FIG. 5

Figure(s)

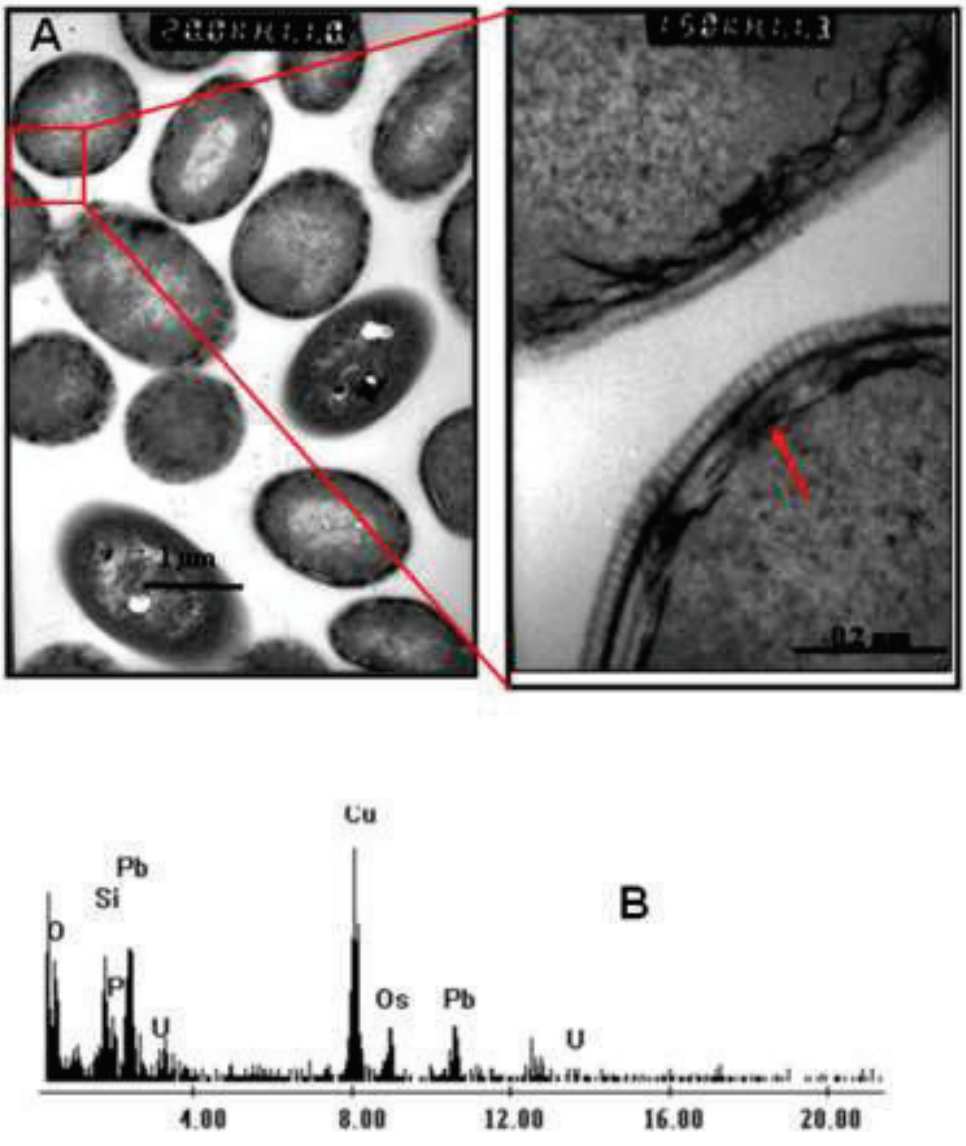

FIG. 6

Figure(s)

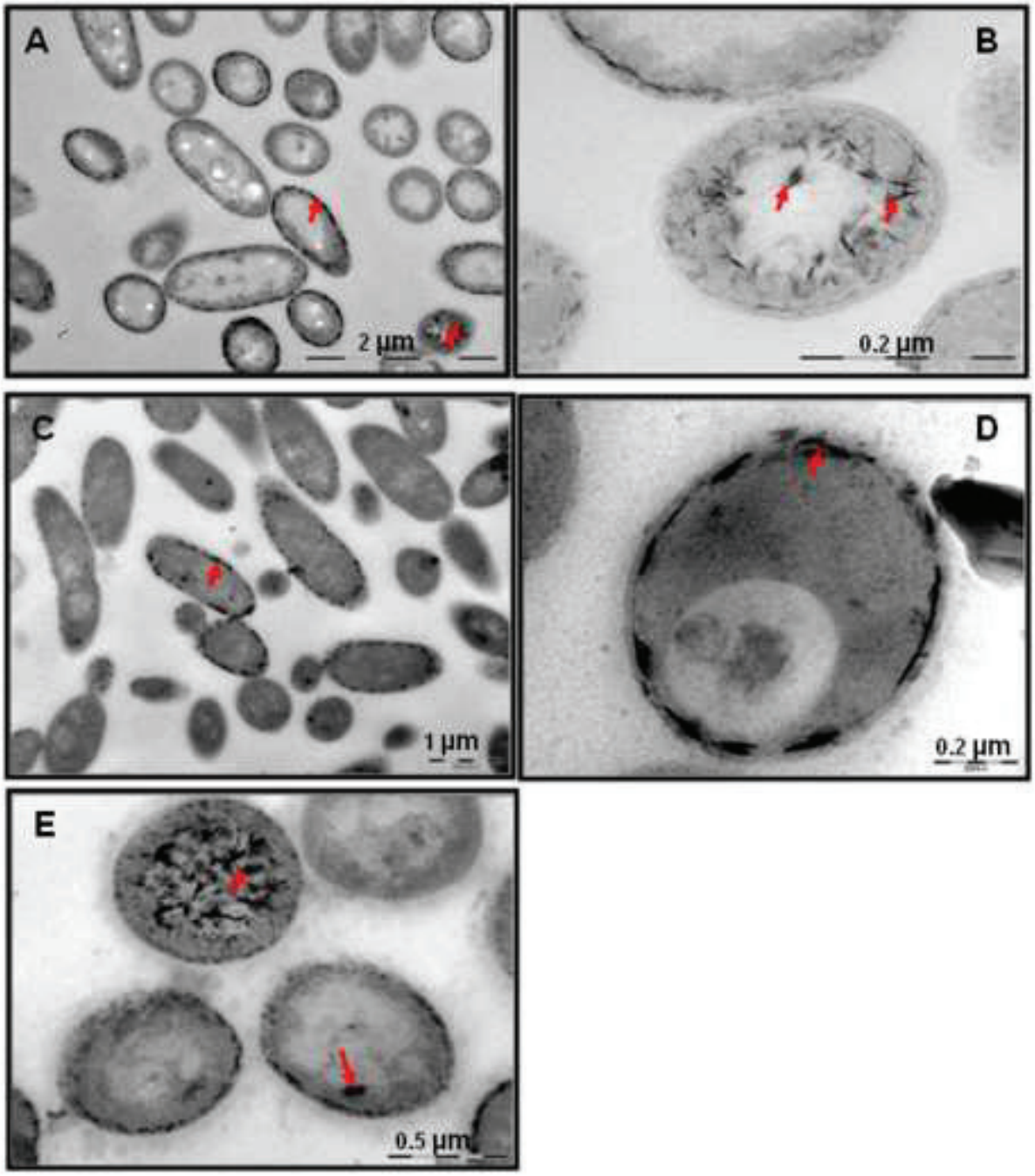

FIG. 7

Figure(s)

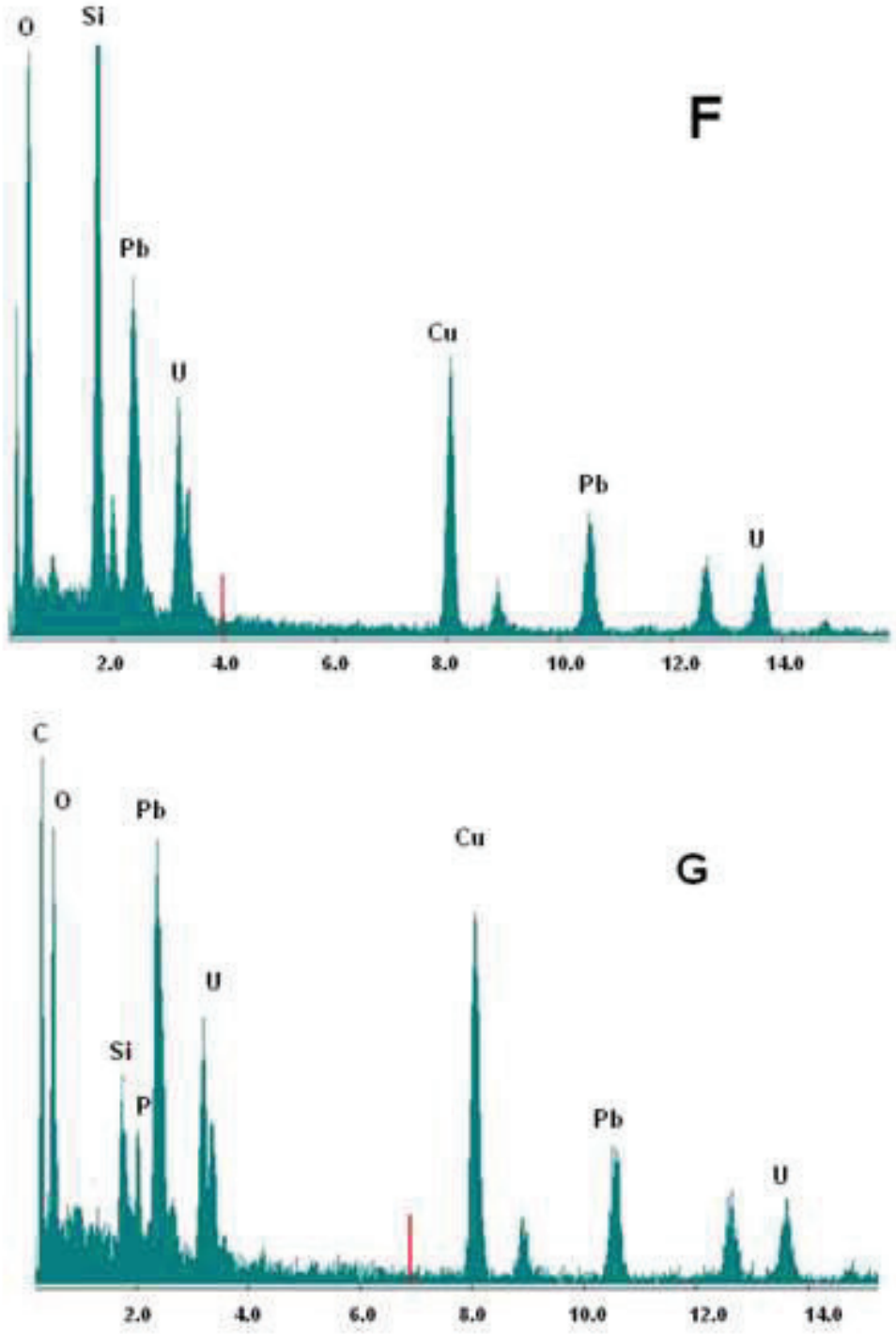

FIG. 7

figure(s)

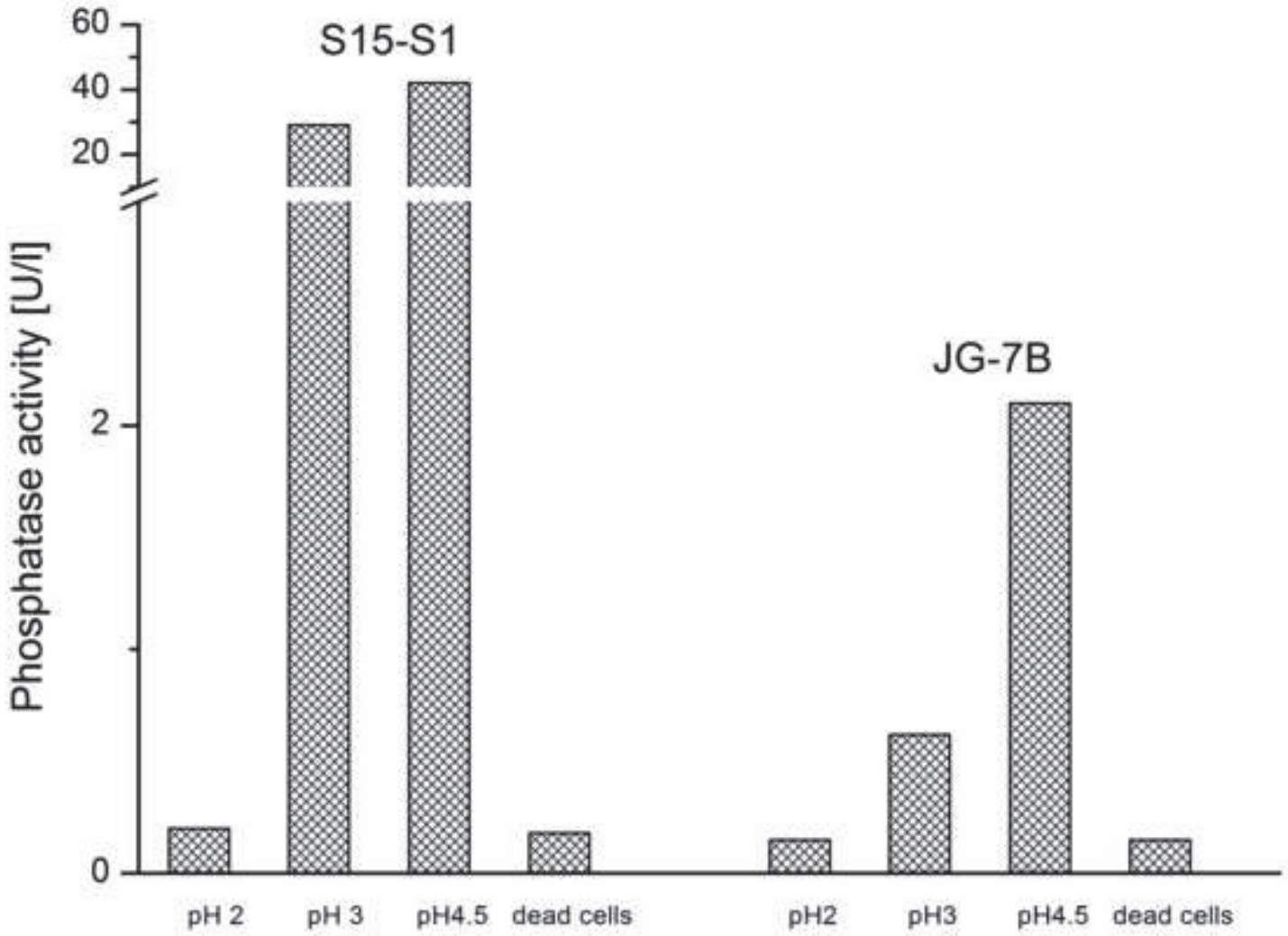
S15-S1
JG-7B
Phosphatase activity [U/l]
60
40
20
2
0
pH 2
pH 3
pH4.5
dead cells
pH2
pH3
pH4.5
dead cells

Figure(s)

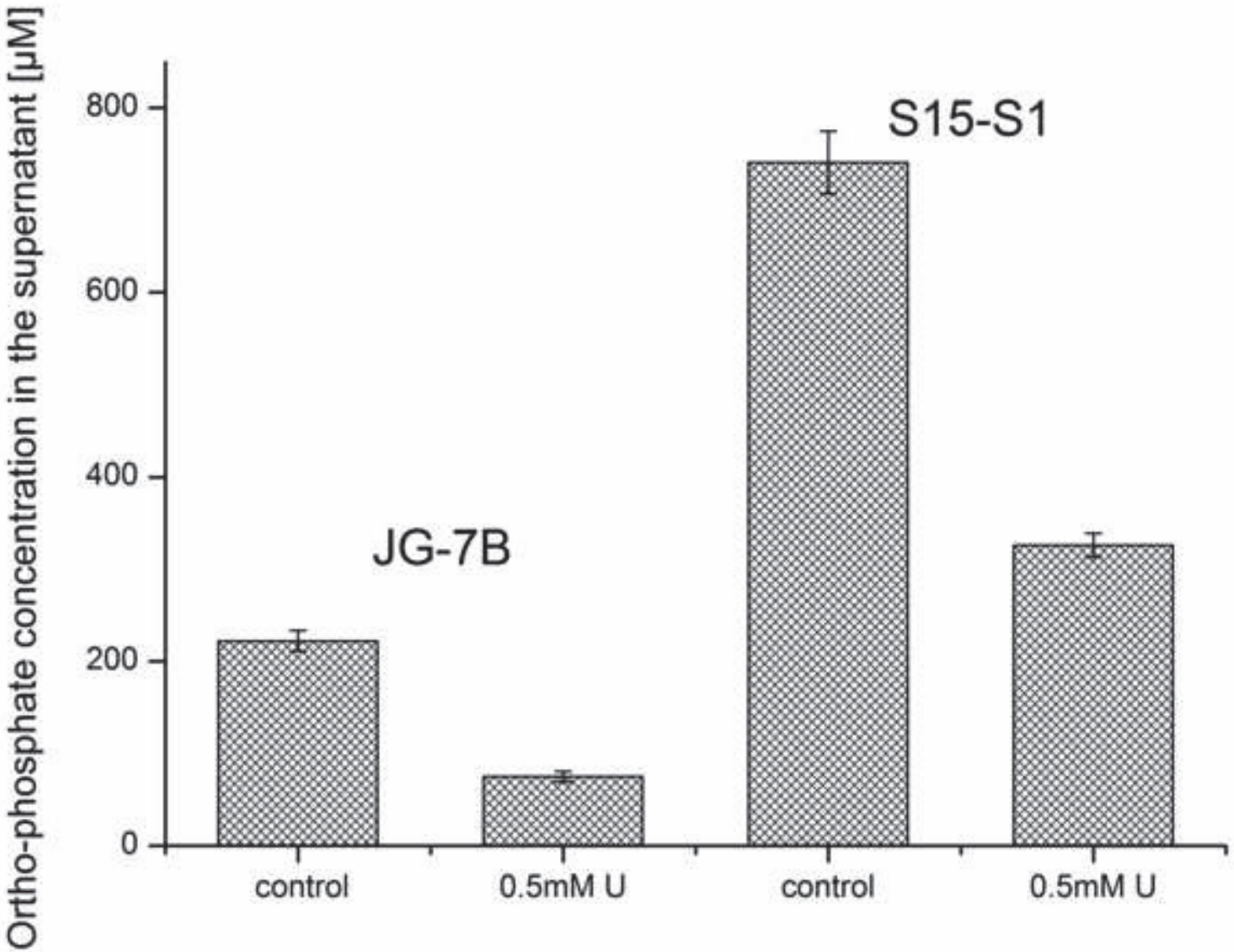
Ortho-phosphate concentration in the supernatant [µM]
800
600
400
200
0
JG-7B
S15-S1
control
0.5mM U
control
0.5mM U